NACA TN 4038

NATIONAL ADVISORY COMMITTEE FOR AERONAUTICS

TECHNICAL NOTE 4038

PERFORATED SHEETS AS THE POROUS MATERIAL FOR A SUCTION-FLAP APPLICATION

By Robert E. Dannenberg, James A. Weiberg,
and Bruno J. Gambucci

Ames Aeronautical Laboratory
Moffett Field, Calif.

Washington
May 1957

B

NATIONAL ADVISORY COMMITTEE FOR AERONAUTICS

TECHNICAL NOTE 4038

PERFORATED SHEETS AS THE POROUS MATERIAL FOR A SUCTION-FLAP APPLICATION

By Robert E. Dannenberg, James A. Weiberg, and Bruno J. Gambucci

SUMMARY

This report gives an account of experiments carried out with a two-dimensional model of an NACA 0006 airfoil with area suction applied on the upper surface near the hinge line of a 0.3-chord plain trailing-edge flap. The distribution of the suction quantity taken into the porous region was controlled generally by means of perforated metal sheets. The permeability of the sheets was controlled by the size and the spacing of the holes. A wide variety of hole sizes and perforation patterns was tested with uniform and gradient arrangements of permeability.

Measurements were made of both the pressure and the suction velocity distributions over the surface of the porous region for each permeability arrangement tested for a range of suction flow extending from no flow to a value well above that required for separation control over the flap. Further information on the effects of hole size and spacing was provided by use of perforated sheets with a resistance backing to control the inflow distribution. Limits are indicated for the hole size and the hole spacing suitable for the porous region on a suction flap.

INTRODUCTION

One of the problems confronting the designer of a boundary-layer control system using area suction is the selection of a suitable material for the porous area. Two fundamental properties required of the porous material are:

(a) An outer surface which is not detrimental to the aerodynamic characteristics desired.

(b) A permeability which provides the proper control of the suction flow quantities.

Other desirable properties of the material include strength and formability characteristics, ease of attachment, long service life (freedom from clogging by dirt or by corrosion), and ease of reproduction (especially of the flow-resistance characteristics).

A porous material has recently been investigated at the NACA Ames Aeronautical Laboratory which holds particular promise as a practical material for service operation. This material consists of a perforated metal sheet in which the permeability is controlled solely by the size and/or the spacings of the perforations. The permeability and the permeability distribution can be closely controlled to meet the typical specifications for boundary-layer control systems using area suction for lift control (see ref. 1). A study of the functional characteristics of various types of porous materials as reported in reference 2 indicated that perforated sheets tended to clog less than the other materials tested and were the least influenced by corrosive environment. The perforated sheet material had strength and forming characteristics that were superior to sintered powdered materials and comparable to sintered wire materials.

The air flow through a perforated sheet is more concentrated (due to the larger size and smaller number of openings) than that through a woven or a sintered metal sheet. An investigation of the effect of hole size, shape, and spacing on aerodynamic performance was beyond the scope of reference 1 or 2.

The purpose of this report is to present the results of an investigation to determine what hole sizes and spacings can be used effectively without creating adverse aerodynamic effects on high-lift applications using area suction on a trailing-edge flap. (The aerodynamic problems of such an application to swept wings is discussed in ref. 3.) The present investigation used an NACA 0006 airfoil equipped with a 0.3-chord plain trailing-edge flap deflected 50°. A large number of different perforated sheets was tested in the porous region of the flap. The permeability of the porous region was controlled by either (1) the size and/or spacing of the perforations or (2) a second porous material in back of the perforated sheet. The hole patterns of the sheets (and the air-flow resistance of the backing materials) were selected to form various arrangements of uniform and gradient permeability. The tests were made in the Ames 7- by 10-foot wind tunnel and included measurements of surface pressure distributions, lift, and suction requirements.

NOTATION

c chord of model, ft

c_l section lift coefficient, $\frac{\text{lift per unit span}}{q_\infty c}$

c_m section pitching-moment coefficient referred to the quarter-chord point, $\frac{\text{pitching moment per unit span}}{q_\infty c^2}$

c_Q section flow coefficient, $\frac{Q}{V_\infty c}$

d hole diameter, ft

P pressure coefficient, $\frac{p-p_\infty}{q_\infty}$

p local static pressure, lb/sq ft

Q volume flow per unit span (at standard density) through porous surface, cu ft/sec

q_∞ free-stream dynamic pressure, $\frac{1}{2}\rho_\infty V_\infty^2$, lb/sq ft

s center-to-center spacing between adjacent holes in a chordwise row, ft

V_∞ free-stream velocity, fps

v velocity normal to surface calculated from local pressure difference across porous region and flow-resistance characteristics of porous material, fps

w stall-point velocity at the trailing edge of the porous region $\frac{v}{\text{open-area ratio}}$, fps
(For a composite assembly, an equivalent open-area ratio is used and is obtained by interpolation from either figure 2 or 3 of reference 1 using the stall-point values of pressure drop across the assembly and the suction air velocity.)

z center-to-center spacing between adjacent holes in a spanwise row, ft

α angle of attack, deg

δ flap deflection, deg

ρ mass density of air, slugs/cu ft

Subscripts

e local external point

∞ free-stream conditions

1 conditions in suction duct

MODEL AND APPARATUS

The tests were made in the Ames 7- by 10-foot wind tunnel with the test section modified to accommodate a two-dimensional model with a 4-foot span. Figure 1 shows the symmetrically spaced flow dividers which were installed to provide for a 4- by 10-foot test section. Each divider extended about 12 feet forward and rearward from the center line of rotation of the model. A photograph of the 4-foot chord model mounted in the wind tunnel is presented in figure 2. The model was supported on the wind-tunnel balance system. Airfoil-shaped fairings were used to shield the model support structure from the air flow between the flow dividers and the original floor and ceiling of the tunnel test section.

The model used in this investigation was constructed to the profile of an NACA 0006 airfoil with a 0.30-chord trailing-edge flap deflected 50°. The contour of the upper surface of the airfoil above the flap hinge line was an arc of a circle tangent to the airfoil surface with the center of the arc at the 0.70-chord station on the lower surface. The upper surface of the model above the flap hinge line was removable and included provisions for mounting porous sheet materials from 69.0- to 75.7-percent chord. A section view of the model showing the location of the porous area is given in figure 3.

Two arrangements of materials were used in the porous region of the model to control the permeability, that is, the resistance to air flow through the surface. In one arrangement, the porous material consisted of a perforated metal sheet in which the permeability was controlled by the hole size and/or hole spacing. The perforation patterns of sheets used in this manner are shown in figure 4. The air-flow resistance characteristics of the surfaces can be obtained from reference 1 and will not be repeated in this report. Surfaces 1 through 6 with uniform permeability and surfaces 17 through 20 with gradient permeability were perforated only in the region (71.0- to 74.6-percent chord) in which the preliminary test results had shown that suction was required. A typical surface with this perforation arrangement is shown in figure 5(a). Surfaces 7 through 16 were fabricated from factory stock materials (e.g., fig. 5(b)). The chordwise extent and position of the porous region was adjusted by closing off portions of the surface with a

nonporous tape. Surfaces 7 through 15 were also used to obtain various types of hole patterns and spacings by closing off individual holes or rows of holes with a nonporous tape as indicated in figure 5(c).

In the second arrangement, the porous material consisted of a sandwich type of assembly of perforated metal sheets supporting a fibrous-glass compact interior as illustrated in figure 6. Designed to serve as an underlying porous material in composite assembly with a metal skin, the compact provides for precise permeability control (uniform or gradient). Several distributions of the permeability of the fibrous-glass compact were used to obtain various distributions of the suction velocity. Details of the fibrous-glass compacts are given in reference 4.

The suction pressure required to induce flow through the porous surface was provided by an aircraft-type supercharger driven by a variable-speed motor. The suction equipment was located outside the wind tunnel. Air was drawn through the porous section of the flap into the plenum chamber in the model and then through ducting from one end of the model to the supercharger. Baffling was provided in the plenum chamber to insure uniform internal pressures across the span of the model.

Orifices flush with the surface were provided along the midspan of the model and 6 inches from each tunnel wall for determining the chordwise distribution of external pressure. Flush orifices were also installed at various points in the plenum chamber to determine the magnitude and uniformity of the internal suction pressures.

TEST METHODS

Preliminary investigation showed that the use of area suction near the leading edge of the flap increased the lift for all angles of attack. With the largest amount of suction that could be applied with the suction equipment, the lift was well above that of the plain wing and flap combination as shown in figure 7 by the circle symbols but considerably below the lift predicted from the theory of references 5 and 6. Tuft studies indicated a region of rough flow on the flap near the tunnel floor and ceiling. Apparently the reduced pressure on the wing near the hinge line, especially with suction, caused a transfer of some of the boundary layer from the walls to the ends of the flap of the model. Attempts to eliminate or limit the region of rough flow with arrangements of separation plates, fences, turning vanes, or slats over the hinge-line region were unsuccessful.

After further investigation with various blowing and suction slot arrangements in the flap-wall junctures, the regions of rough flow at the ends of the flap were eliminated by increased suction through separate ducts adjacent to the wind-tunnel walls. The results relating

to the flap-wall interference studies are not reported in detail and only the suction arrangement and results pertinent to this investigation will be indicated. Details of the end ducts, which had a quantity flow control independent of the larger span section, are indicated in figure 8. With nominal suction applied to the model, and an increased suction quantity at the end ducts, the lift obtained was nearly equal to the value predicted from theory as indicated in figure 7. Pressure-distribution studies showed a pressure recovery at the trailing edge of the flap that was uniform across the span and that was of the type associated with a two-dimensional air stream. Tuft photographs are shown in figure 9. For a section flow coefficient in each end duct of 0.02 or less (based on total model wing area), the lift coefficient varied between the two curves shown in figure 7 for the suction-applied conditions. Increased suction in the end ducts of 0.02 or greater did not affect the lift or stall-point c_Q within the accuracy of measurement. The lift with suction off shown in figure 7 was not affected by the quantity of the suction flow into the end ducts.

In this report, all force and flow data are presented for a constant section flow coefficient in the end ducts which was sufficient to insure a two-dimensional type of flow about the model. The section flow coefficient c_Q given on the figures refers to the suction flow quantity applied to the remainder of the porous area, that is, it does not include the flow in the end ducts.

Measurements of the lift and pitching moment were made with the wind-tunnel balance system. Tunnel-wall corrections computed by the method of reference 7 were applied to the data as follows:

$$\alpha = \alpha_u + 0.30\, c_{l_u} + 1.22\, c_{m_u}$$

$$c_l = 0.96\, c_{l_u}$$

$$c_m = 0.99\, c_{m_u} + 0.01\, c_{l_u}$$

where the subscript u denotes uncorrected values. Unless otherwise noted all tests were made for a free-stream velocity of 162 feet per second (Mach number of 0.14) which, for the 4-foot chord of the model, corresponded to a Reynolds number of 4,000,000.

The weight rates of air flow through the end ducts and through the porous region of the flap were measured independently by means of standard A.S.M.E. orifices. The flow-resistance characteristics of the porous materials were ascertained experimentally by the method described in reference 1. The data presented for the suction-off condition ($c_Q = 0$) were obtained with the suction lines sealed between the model and the suction pumps.

RESULTS

Effects of Suction

A preliminary series of tests were made on the NACA 0006 airfoil with area suction near the leading edge of the trailing-edge flap to establish the location and chordwise extent of the porous region necessary for efficient lift control. These tests were exploratory in nature with the object of gaining both an understanding of the suction requirements and ascertaining the lift potentialities of the model arrangement.

A trailing-edge flap acts to change effectively the camber of the airfoil section. From the data in reference 8, it can be noted that for deflections up to approximately 15° or 20°, the flow over the flap is attached and the increase in lift due to flap deflection agrees with values computed from thin-airfoil theory. With increasing flap deflection above 20°, however, the flow separates from the flap, resulting in a lift well below the predicted value. This flow separation is indicated in figure 10(a) by the relatively constant pressures over the rear of the flap. Because of this flow separation, the peak pressure coefficients over the hinge-line region on the flap did not exceed a value of about -2.

The application of suction in the hinge-line region on the upper surface prevented flow separation and resulted in more negative pressure coefficients on the flap, as is shown in figure 10(b). The location of the peak pressure, however, remained at approximately 71.0-percent chord. The lift approached that predicted from theory as shown in figure 7.

To determine where the porous region on the upper surface of the flap should be positioned in order to obtain a maximum of lift for the least suction quantity, tests were made with various chordwise extents and locations of the porous region. The results indicated that the position of the porous region was related to the external pressures over the flap. It was found that a porous region located between 71.0- and 74.6-percent chord was required to control the lift with a minimum quantity of suction air. Increasing the chordwise extent of the porous boundaries resulted in an increase in c_Q without any change in lift. The upstream edge of the porous region was found to coincide with the point of minimum pressure on the flap. The downstream edge was at the chordwise station at which the more or less large adverse pressure gradient over the porous region abruptly became less positive and the external pressure coefficient had recovered to a value of about -1.5.

With a high suction flow rate and the lift at a value close to that predicted from theory, the pressures near the trailing edge of the flap were near or slightly above the free-stream static pressure, indicating attached flow over the flap. As the c_Q was gradually reduced,

the pressures near the trailing edge of the flap decreased slightly with the onset of separation of the turbulent boundary layer from the trailing edge of the flap (see fig. 11(a)). Further decrease in c_Q eventually caused an abrupt loss in lift as the suction quantity reached a value insufficient to control separation near the hinge line. For the purpose of this report, the lowest flow coefficient required to maintain unseparated flow over the hinge-line region of the flap will be referred to as the stall-point c_Q.

The section flow coefficient required to maintain attached flow at the trailing edge of the flap is also of interest. This quantity is discussed and designated in reference 3 as $c_{Q_{crit}}$. In this report, the lowest flow coefficient required to maintain unseparated flow at the 95-percent chord station on the upper surface of the flap will be referred to as the critical-point c_Q (see fig. 11(a)).

The lift and pitching-moment characteristics shown in figure 11(b) were obtained with a surface which was uniformly permeable in the porous region (surface 4, fig. 4). Except for the values of c_Q, these data are typical of the lift and moment characteristics noted with different distributions of permeability of the material in the porous region for values of c_Q greater than the stall point. The value of the stall-point c_Q changed with the permeability (uniform or gradient) of the porous region. The effect of permeability distribution on the stall-point c_Q will be discussed in the following section.

Effects of Hole Size and Spacing

Uniform permeability.- The lift and flow characteristics of the model were obtained with each of the surfaces shown in figure 4(a) installed in the porous region. The perforation pattern of each sheet had about the same ratio of hole spacing (center-to-center) to hole diameter in the chordwise as in the spanwise direction (i.e., $z/d \approx s/d$). The open-area ratio, however, ranged from 0.6 percent up to 41 percent. In addition, data were obtained with a full-open porous region from 71.0- to 74.6-percent chord (100-percent open).

As a porous material, perforated sheets have a wide range of permeability and can be made to almost any desired uniform or gradient arrangement (see ref. 1). In order to give an indication of the permeability of the different surfaces in figure 4(a), a permeability relative to that of surface 1 has been tabulated in the figure. This relative permeability is the ratio of velocities of air flow induced for a pressure difference of 10 inches of water across the sheets.

In figure 12, the lift, section flow, and plenum chamber pressure coefficients at the stall point (and critical point) are presented as a function of the open-area ratio of the perforated surfaces used in the

porous region. The trend of the data presented in figure 12 is not dependent on the individual perforation patterns themselves, but rather indicates the over-all effects of permeability on the aerodynamic characteristics of the model. It can be readily noted that the section flow coefficient at the stall point was decreased by a factor of about 4 as the open area of the porous region was decreased from 100 to 2 percent.

With a 1-percent open area (surface 2), the largest differential of suction pressure that could be applied with the suction equipment was insufficient to attach the flow over the flap at the test conditions (V_∞ = 162 fps). Reducing the free-stream velocity to 94 feet per second increased the available section flow coefficient as noted below and resulted in attached flow over the flap. With a 0.6-percent open area (surface 1), the flow was not attached by reducing the free-stream velocity.

Open area of porous region, percent	V_∞, fps	c_l ($\alpha = -15^\circ$)	c_Q	P_1
1.0	162	1.00	0.0008	-21
1.0	132	1.18	.0011	-33
1.0	94	1.54	.0014	-61
.6	94	.69	.0008	-56

Discrete permeability.- In order to determine the largest hole spacing for a given hole size that would provide for efficient lift control on the flap, various surfaces were modified by taping over portions of the skin to obtain a more or less systematic variation of s/d and z/d. The suction quantity was concentrated at several chordwise stations rather than distributed over the porous region. These arrangements are designated as having a discrete permeability.

The effects of discrete permeability in the porous region were studied with surfaces having hole diameters of 0.045, 3/32, 1/8, 3/16, and 1/4 inch. Typical results are presented in figure 13 for surface 13 with 1/8-inch-diameter holes. Illustrated in figure 14 are the variations in suction quantity versus suction pressure for various permeability arrangements. Evaluation of the data shown in figures 13 and 14 and other similar data obtained with surfaces having different sized holes indicated that as the permeability of the porous region was decreased by closing off some of the holes, the stall-point c_Q also decreased. It was found that if the hole spacings for a given hole size were kept within certain limits, the variation of the stall-point c_Q with open-area ratio was the same as that noted for surfaces having uniform permeability as indicated in figure 12.

The lift and the c_Q at the stall point for each discrete permeability pattern were compared with the values indicated in figure 12 for surfaces having equal open area but of uniform permeability. Those perforation patterns for which the lift and c_Q were the same as the

values from figure 12 were considered as satisfactory and are indicated in figure 15. With certain patterns, the lift was the same but the stall-point c_Q was greater than the value from figure 12 for equal open area. This range of patterns is shown by the shaded areas in figure 15. Further increase in the hole spacing, either chordwise or spanwise, resulted in a separated flow over the flap hinge line that could not be eliminated even with the maximum suction quantity through the porous region. These patterns fall within the region labeled "stalled" in figure 15.

It is interesting to note that a porous surface having two spanwise rows of holes, at about 71.0- and 74.6-percent chord, respectively, had practically the same aerodynamic control (i.e., the same c_l and c_Q characteristics) as a porous surface with many rows of spanwise holes between the same two chordwise stations (compare, e.g., surface 13-E of fig. 13 with surface 6 of fig. 4).

A slight hysteresis was noted for the pattern arrangements with only two spanwise rows of holes. The stall point for two arrangements (13-E and 11-A) was obtained by gradually reducing c_Q until the flow over the flap separated. Once the model stalled, the c_Q had to be increased by about 0.001 over the stall-point value before the flow was reattached. It should be noted, however, that the ratio of hole spacing to hole diameter for arrangements 13-E and 11-A was in the increased stall-point c_Q range as indicated in figure 15. Therefore, the hysteresis noted above may not be a result of using two rows of holes but may have been a result of the holes being spaced too far apart. No arrangement of two rows of holes tested was in the range indicated as satisfactory in figure 15. With any of the patterns indicated as satisfactory in figure 15 installed in the porous region, the value of the stall-point c_Q was found to be independent of the manner in which the suction quantity was varied.

Gradient permeability.- For the uniform and the discrete arrangements of permeability, the hole size and spacing pattern (s/d and z/d) were constant throughout each individual surface. By the use of non-uniform perforations, that is, unequal hole sizes and/or variable spacings, a perforated sheet can be made to a prescribed gradient arrangement of permeability. Four surfaces of this type with the same gradient permeability but with different hole sizes and spacings were tested and are illustrated in figure 4(b). Surfaces 17, 18, and 19 had a given hole size with different spacing patterns. Surface 20 had a uniform spacing pattern with different hole sizes in the rows. The variation of c_Q with P_1, and the stall-point c_Q for each of these surfaces were the same (see fig. 14(b)).

In certain applications, the use of surface sheets with open areas up to 30 or 40 percent may be desirable. To be able to use these more open sheets and still maintain a prescribed permeability arrangement (e.g., the requirements diagramed in fig. 4(b)), the porous-flow resistance must be increased selectively. A number of surfaces were

tested with a resistance backing as shown in figure 6. The over-all gradient permeability was the same as that for surfaces 17 through 20.

The stall-point c_Q for the materials with gradient permeability in the porous region are shown in figure 16. The result to be noted is that the stall-point c_Q (with equal gradient permeability) was not affected by the perforation patterns of the surface material. The porous region formed by a sheet with 0.125-inch-diameter holes, 33 holes per square inch, was equivalent aerodynamically to a sheet with 4,225 holes per square inch and 0.006-inch square holes.

Pressure distribution.- For perforated surfaces (uniform permeability) with open areas of about 6 percent or larger, some outflow occurred near the leading edge of the porous region even for section flow coefficients greater than that required at the stall point. The chordwise extent of outflow in the porous region at the stall point with an open area of 41 percent (surface 15) was large, as can be deduced from figure 17. From the flat-top shape of the pressure distribution, it appeared that outflow caused a localized flow separation over the forward portion of the porous region. However, the high suction quantities taken through the trailing-edge region appeared to reattach the flow and limit the local separation. As the permeability of the porous region was decreased, the region of outflow also decreased and the shape of the pressure diagrams changed as can be seen in figure 17.

The shape of the pressure diagrams at the stall point for the discrete arrangements of permeability with small open-area ratios and the tapered arrangements of permeability were essentially the same as that shown for surface 4 in figure 17.

DISCUSSION

An extensive selection of perforation patterns with a wide range of hole sizes and spacings is available to a designer for a suction flap system which will produce essentially the same aerodynamic result (see fig. 15). The stall-point c_Q was found to vary according to the permeability of the material used in the porous region (see figs. 13 and 16). Highly permeable materials resulted in large values of stall-point c_Q. More dense materials, with uniform or gradient arrangements of permeability, resulted in a reduction in the stall point c_Q. In an attempt to correlate the results obtained in terms of the suction requirements for attached flow on the flap, examination was made of the suction velocity distribution at the stall point with attached flow. A number of velocity distributions corresponding to the stall-point values for materials of different permeability are shown in figure 18. Inspection of this figure reveals two significant features regarding the distribution of local suction velocities required to prevent separation: First, the attainment of attached flow on the flap was insensitive to the velocity of flow through the leading edge of the porous region. The

velocity could be varied from large inflow values to even considerable outflow and still maintain attached flow on the flap. Second, at the trailing edge of the porous region a positive value of suction velocity was always necessary for attached flow on the flap but it did not appear to have any specific value; however, the magnitude of the velocities did appear to be related to the permeability of the surface at that point.

A considerable effort was made to establish the sensitivity of the stall-point c_Q to the magnitude and location of the velocity at the trailing edge of the porous region. In all instances, moving the chordwise position of the trailing edge of the porous region away from 74.6-percent chord (±0.3-percent chord) was harmful. Positions upstream resulted in an inability to prevent flow separation. Positions downstream resulted in an increased suction quantity at the stall point. The location of the trailing-edge position appeared to be related to the chordwise station at which the more or less large adverse pressure gradient over the porous region abruptly became less positive (see fig. 17).

It was noted from examination of the suction velocity diagrams, at the stall point, for all the permeability arrangements tested, that the suction velocity[1] v at the trailing edge of the porous region varied considerably with the permeability of the porous material. Plotting this suction velocity as a function of the open area of the porous region resulted in a linear variation. The velocity of the air into the perforations would be greater by the ratio of the total area to the open area of the perforations. This velocity w of the suction air through the perforations at the trailing edge of the porous region was found to be essentially a constant value at the stall point and to be independent of the permeability of the porous region as shown in figure 19(a). The data in figure 19(a) represent a wide range of stall-point c_Q values. The agreement was as good for the perforated sheet materials used alone as for sheets used with a resistance backing.[2] It was clear that separation was suppressed for any arrangement of surface permeability provided the magnitude of the suction velocity through the perforations at the trailing edge of the porous region was equal to or greater than some critical value at the stall point. The magnitude and distribution of the suction velocities over the forward portion of the porous region influenced the magnitude of the suction quantity c_Q, but did not affect the critical velocity w at the trailing edge.

The variation with free-stream velocity of the velocity w through the perforations at the trailing edge of the porous region is indicated

[1]Suction air velocity, normal to surface, is based on the total surface area of the porous region (71.0- to 74.6-percent chord).

[2]The equivalent open-area ratio of a composite assembly (i.e., a single perforated sheet with the same values of pressure drop and suction velocity) was determined from the stall-point values of pressure drop and suction velocity at the trailing edge of the porous region by interpolation from either figure 2 or 3 of reference 1.

in figure 19(b). It can be noted that the value of w increased with increasing free-stream velocity; however, the ratio w/V_∞ (and hence the stall-point c_Q) was essentially invariant with V_∞.

Wind-tunnel tests of area suction applied at the leading edge of a partial-span flap on a 35° sweptback wing are reported in reference 3. Three arrangements of permeability were tested in the porous region that suppressed separation on the flap. The corresponding suction velocity distributions at the stall point (from fig. 27, ref. 3) are diagramed in the adjacent sketch. The calculated values of w for curves (a), (b), and (c) were 222, 233, and 225, respectively. The results of the two different model installations, reference 3 and that of this investigation, appear complementary in substantiating the sensitivity of the velocity at the trailing edge of the porous region. The test results of reference 3 also indicated that the stall-point c_Q was essentially independent of V_∞.

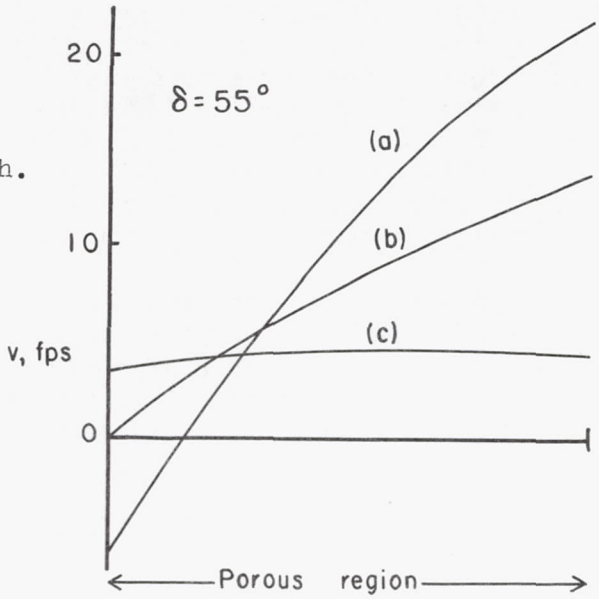

From these two experiments a single parameter appeared dominant in suppressing separation on the flap by suction. This parameter was the suction velocity based on the area of the perforations at or near the trailing edge of the porous region. It appeared to be limited only by certain geometric restrictions to the hole-spacing pattern. Attempts to relate the parameter, w/V_∞, with wing geometry and flap deflection indicated that the correlation obtained depended upon the component of the free-stream velocity normal to the flap and the turning angle near the hinge line of the flap defined as the angle between the wing reference plane and the upper surface of the flap.

The observed sensitivity of the location of the trailing edge of the porous area and the basic importance of the suction velocity at this location suggest the following interpretation of the present method of suppressing separation. The large suction velocity into the perforations at the trailing edge of the porous area (of similar magnitude to the local velocity over the flap immediately downstream of this point) would provide a strong sink effect. The pressure field induced by a sink in an airfoil surface has negative pressures ahead of the sink and positive pressures behind the sink. Thus, if the sink is a short distance behind the knee of the flap, these sink induced pressures could combine with the pressure field of the deflected flap to produce a broadened pressure peak followed by an abrupt recovery. This is apparent in the pressure distributions in figure 17. By proper positioning of the suction, most

of the recovery can be localized at the point at which most of the suction is applied. This suggests the possibility of suppressing separation by applying suction at this single chordwise location. From the results of the data obtained with two spanwise rows of holes, it appears that a single row of spanwise holes properly positioned may be sufficient to control the flow over the flap on the model of this investigation. At the stall point for surfaces 11-A and 13-E (fig. 14), almost all the suction quantity was taken through the downstream row of holes. Across the upstream row, the pressure difference measured between the external and plenum-chamber pressures was zero, indicating no inflow. In fact, for surface 11-B, zero inflow in the upstream row of holes was indicated for a P_1 of about -9 whereas the stall point did not occur until the plenum-chamber pressure coefficient was increased to -7.8, indicating a sizable outflow at the stall point. Further investigation of this possibility appears to be an interesting task for future research.

The use of perforations need not be restricted solely to the application of separation suppression on a plain flap for high-lift control. It is believed that the same concepts could be used advantageously to eliminate flow separation in other aerodynamic systems, for example, in wide angle diffusers, elbows, and bluntly rounded trailing-edge sections.

CONCLUDING REMARKS

The results of a wind-tunnel investigation of an NACA 0006 airfoil with a plain trailing-edge flap indicated that flap lift increments approaching those computed from thin-airfoil theory can be obtained with small suction flow quantities through a porous region on the upper surface near the hinge line of the flap.

A porous region with a perforated metal skin was entirely satisfactory for achieving efficient lift control. The lift gains and the suction quantity requirements were unaffected by the perforation patterns of the porous surface over a wide range of hole sizes and spacings. A perforated surface with its permeability controlled solely by the hole size and spacing was equally as good aerodynamically as a more open surface with a resistance backing. It was shown that a designer has a wide choice in selecting a perforation pattern or distribution of permeability to provide for efficient lift control. Acceptable geometric limitations to hole size and spacing are indicated.

Ames Aeronautical Laboratory
National Advisory Committee for Aeronautics
Moffett Field, Calif., March 14, 1957

REFERENCES

1. Dannenberg, Robert E., Gambucci, Bruno J., and Weiberg, James A.: Perforated Sheets as a Porous Material for Distributed Suction and Injection. NACA TN 3669, 1956.

2. Anon.: Evaluation of Porous Materials for Boundary-Layer Control. WADC Tech. Rep. 56-486, Sept. 1956.

3. Cook, Woodrow L., Holzhauser, Curt A., and Kelly, Mark W.: The Use of Area Suction for the Purpose of Improving Trailing-Edge Flap Effectiveness on a 35° Sweptback Wing. NACA RM A53E06, 1953.

4. Dannenberg, Robert E., Weiberg, James A., and Gambucci, Bruno J.: A Fibrous-Glass Compact as a Permeable Material for Boundary-Layer-Control Applications Using Area Suction. NACA TN 3388, 1955.

5. Glauert, H.: Theoretical Relationships for an Aerofoil with Hinged Flap. R. & M. No. 1095, British A.R.C., Apr. 1927.

6. Keune, A.: Lift on a Bent Flat Plate. NACA TM 1340, 1955.

7. Allen, H. Julian, and Vincenti, Walter G.: Wall Interference in a Two-Dimensional-Flow Wind Tunnel with Consideration of the Effect of Compressibility. NACA Rep. 782, 1944.

8. Gambucci, Bruno J.: Section Characteristics of the NACA 0006 Airfoil with Leading-Edge and Trailing-Edge Flaps. NACA TN 3797, 1956.

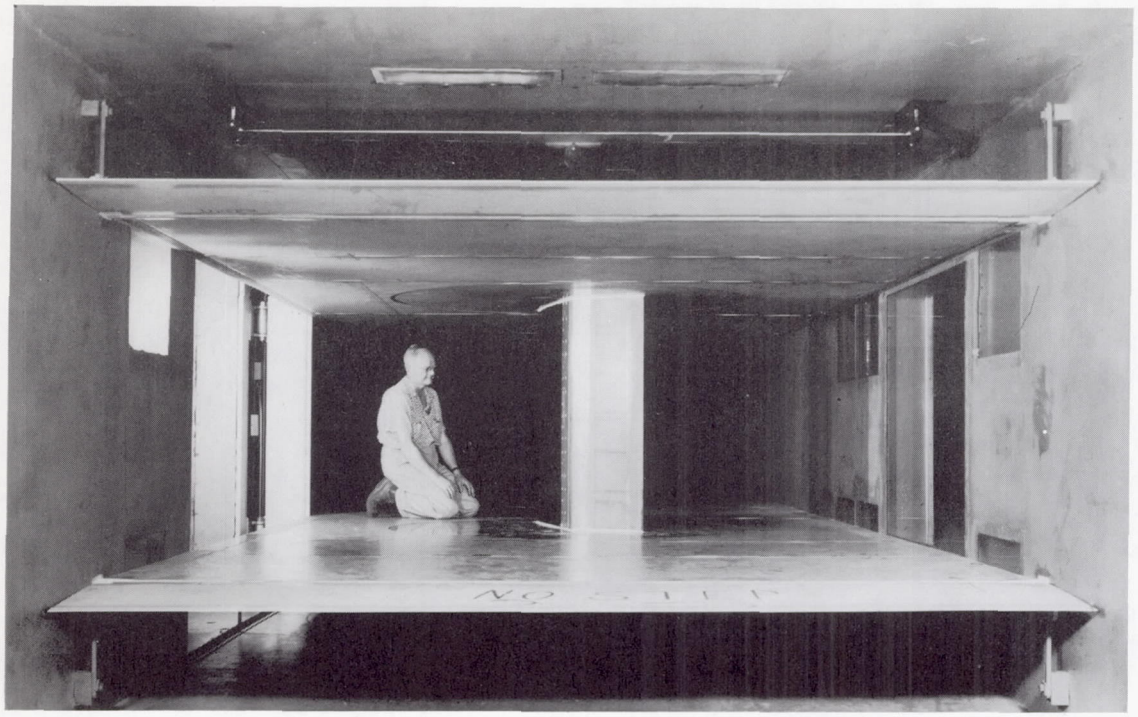

A-20413

Figure 1.- Rear view of the horizontal dividers installed in the 7- by 10-foot wind tunnel to provide a 4- by 10-foot test section.

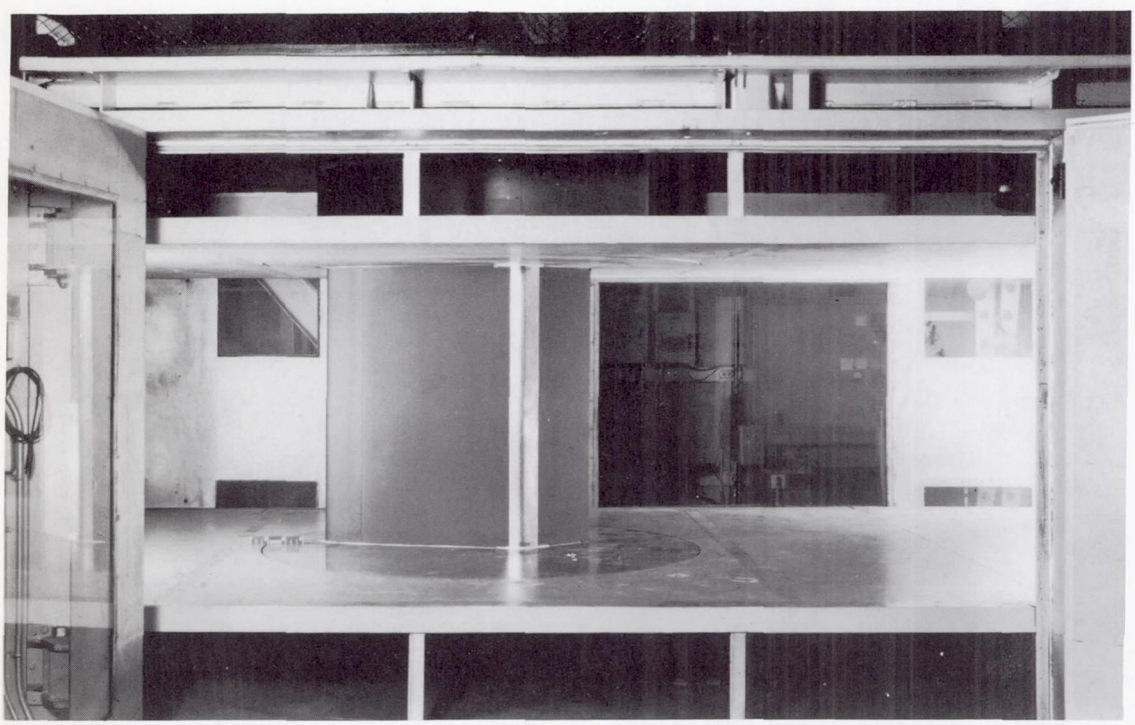

A-21413

Figure 2.- The model installed in the 4- by 10-foot test section.

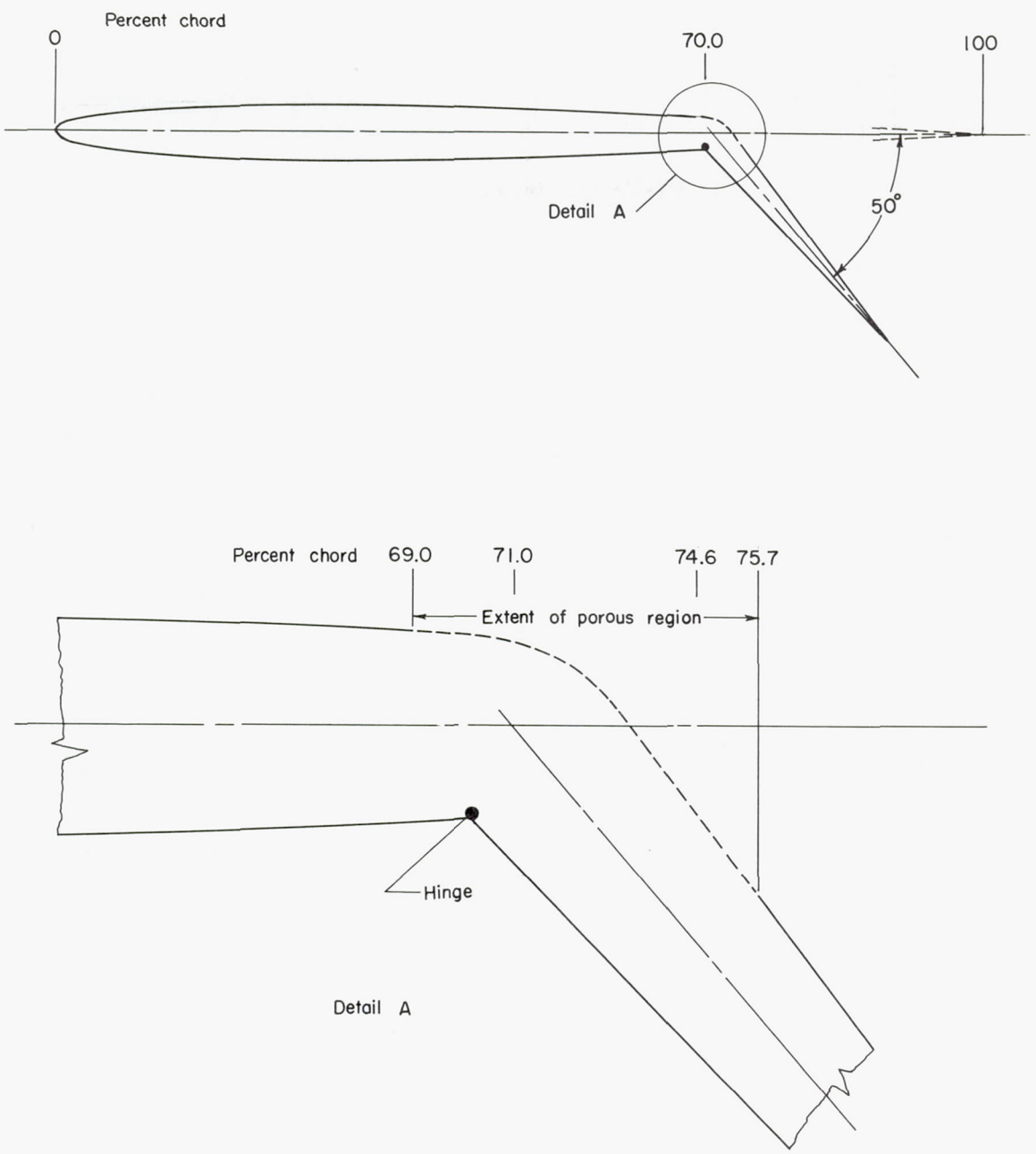

Figure 3.- Location of the porous region on the flap.

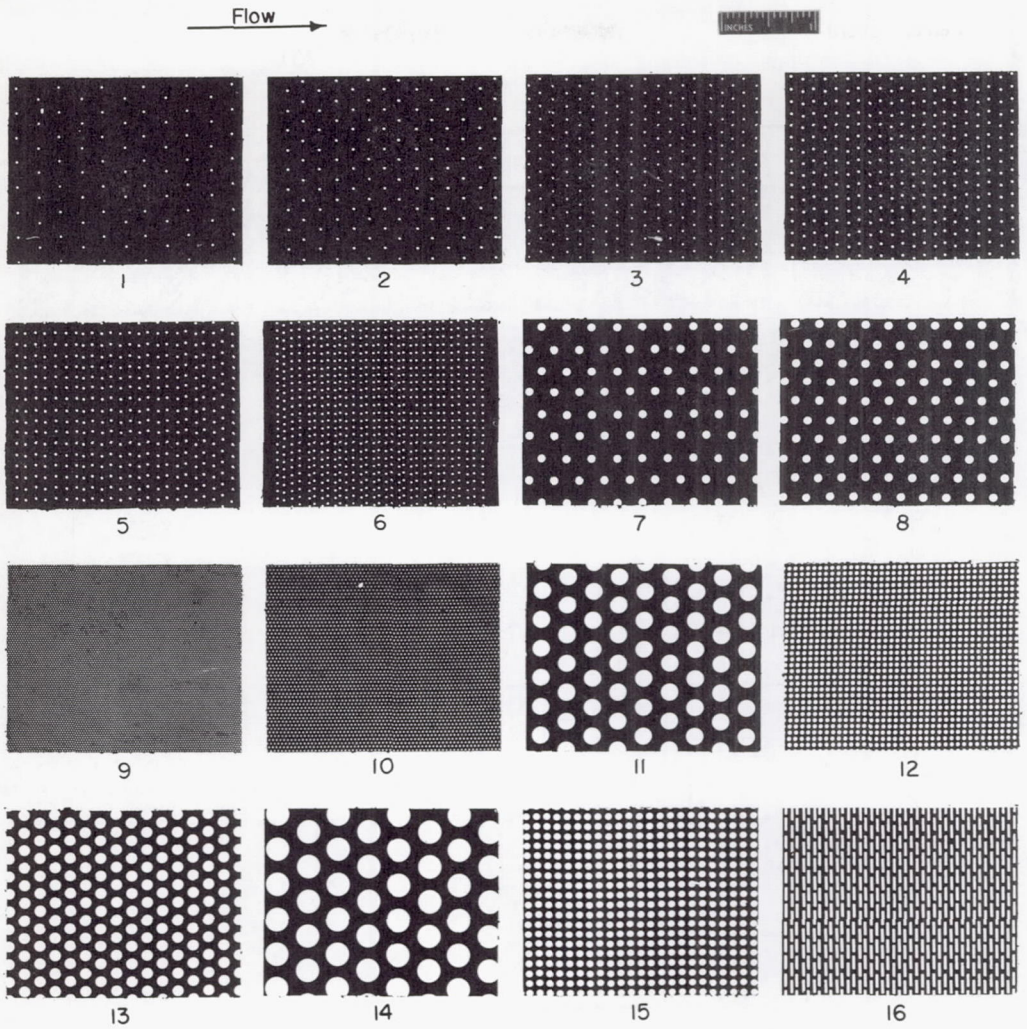

Surface	Hole diam., in.	Holes per sq in.	Percent open	Thickness, in.	Permeability of surface / Permeability surface 1
1	0.023	14.5	0.60	0.016	1
2	.023	24.1	1.0	.016	2
3	.023	47	2.0	.016	4
4	.026	57.6	3.0	.016	6
5	.026	73.7	3.9	.016	7
6	.023	134	5.6	.016	11
7	.094	15.7	10.9	.040	19
8	.094	18	13	.016	22
9	.009	1500 (approx)	15	.0075	20
10	.020	714	≠3	.016	36
11	.187	12	32	.032	67
12	.045	233	37	.016	78
13	.125	33	40	.032	78
14	.250	8.1	40	.036	78
15	.079	83	41	.016	78
16	Slot 0.020 × 0.115	140	30	.016	65
			100		350

(a) Uniform permeability.

Figure 4.- Details of perforation patterns of various metal sheets used in the porous region of the model.

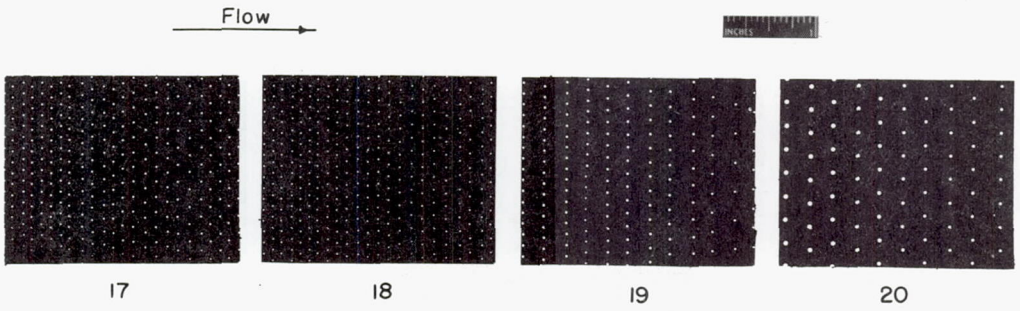

Surface	Hole diam., in.	Number of rows	Percent open	Thickness, in.
17	0.020	24	3.1 to 1.7	0.025
18	.020	23	3.1 to 1.7	.025
19	.029	12	3.1 to 1.7	.025
20	.050 to .036	10	3.1 to 1.7	.025

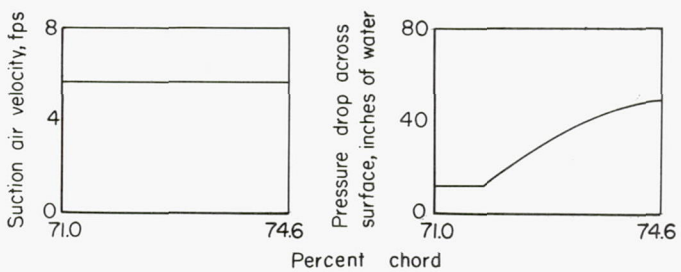

Design condition of pressure drop and suction velocity for surfaces 17 through 20.

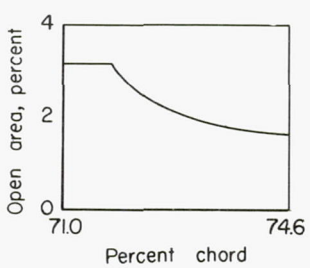

Average open – area distribution corresponding to the design condition.

(b) Gradient permeability.

Figure 4.- Concluded.

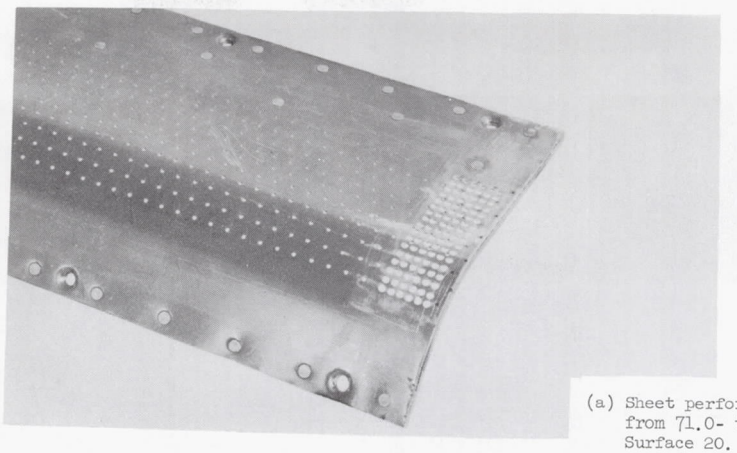

(a) Sheet perforated for porous region from 71.0- to 74.6-percent chord. Surface 20.

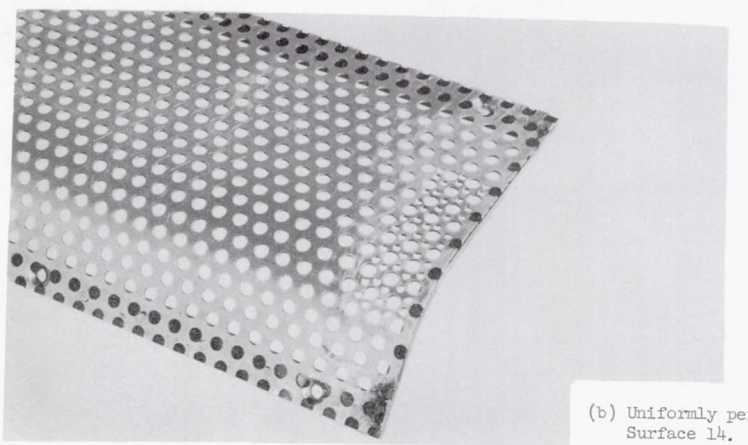

(b) Uniformly perforated sheet. Surface 14.

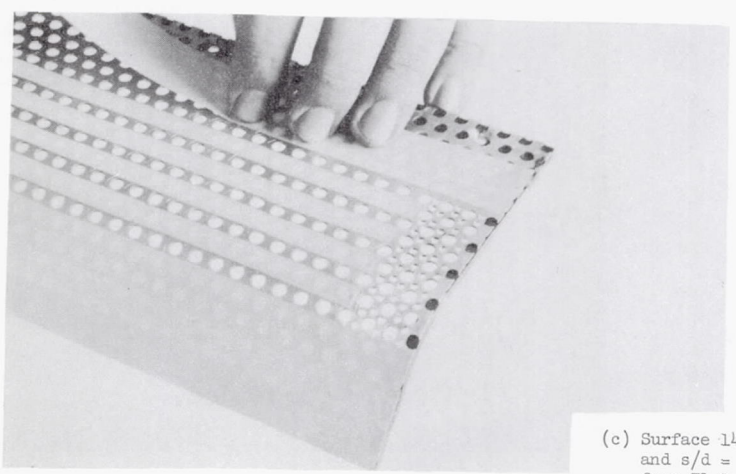

(c) Surface 14 taped for $z/d = 1.66$ and $s/d = 2.88$ for porous region from 71.0- to 74.6-percent chord.

Figure 5.- Typical perforation arrangements tested with different types of surface sheets. The portion of the sheets with the added perforations were open to separate end ducts.

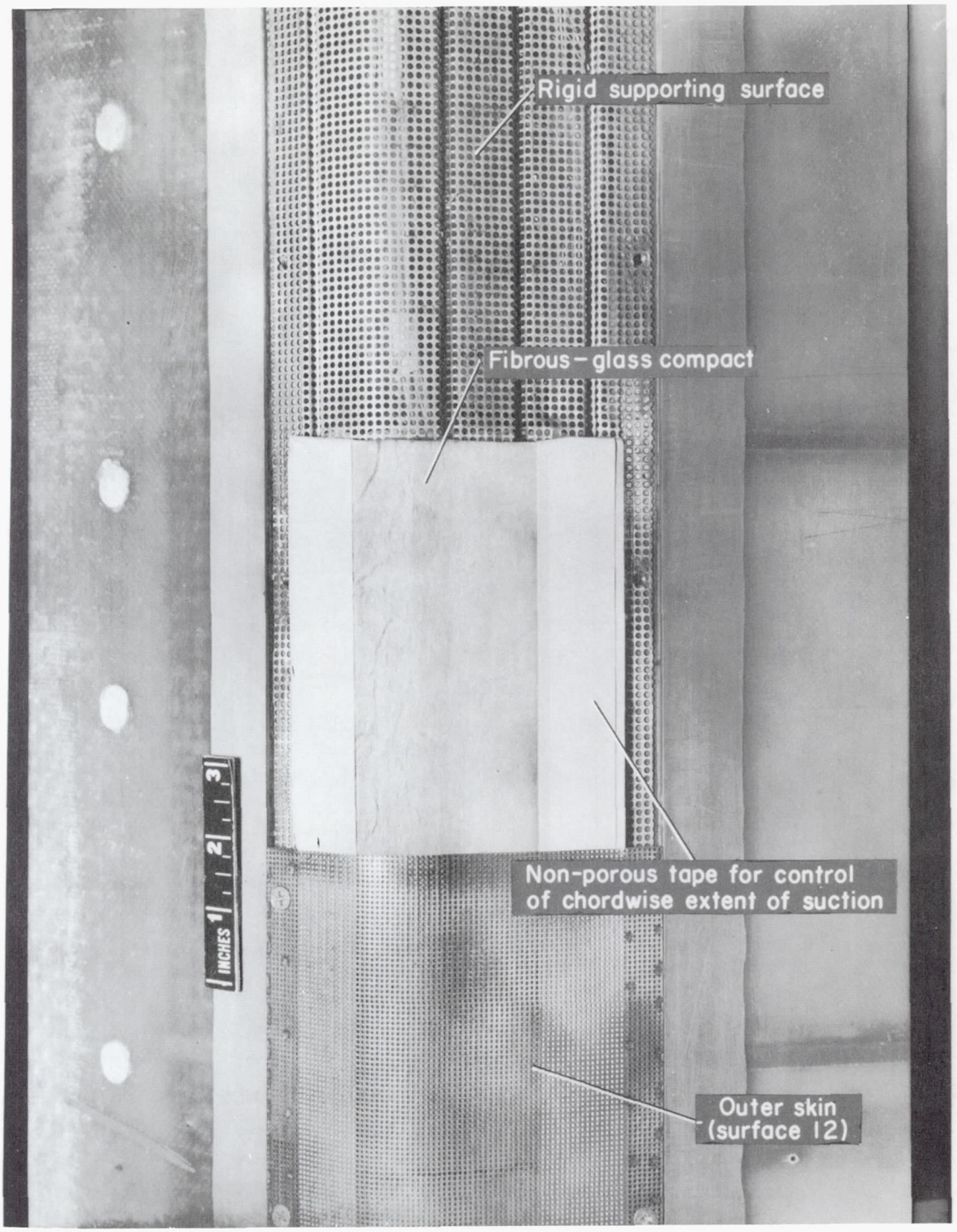

A-21291.1

Figure 6.- Cutaway detail of sandwich type of assembly of perforated sheets and fibrous-glass compact in the porous region.

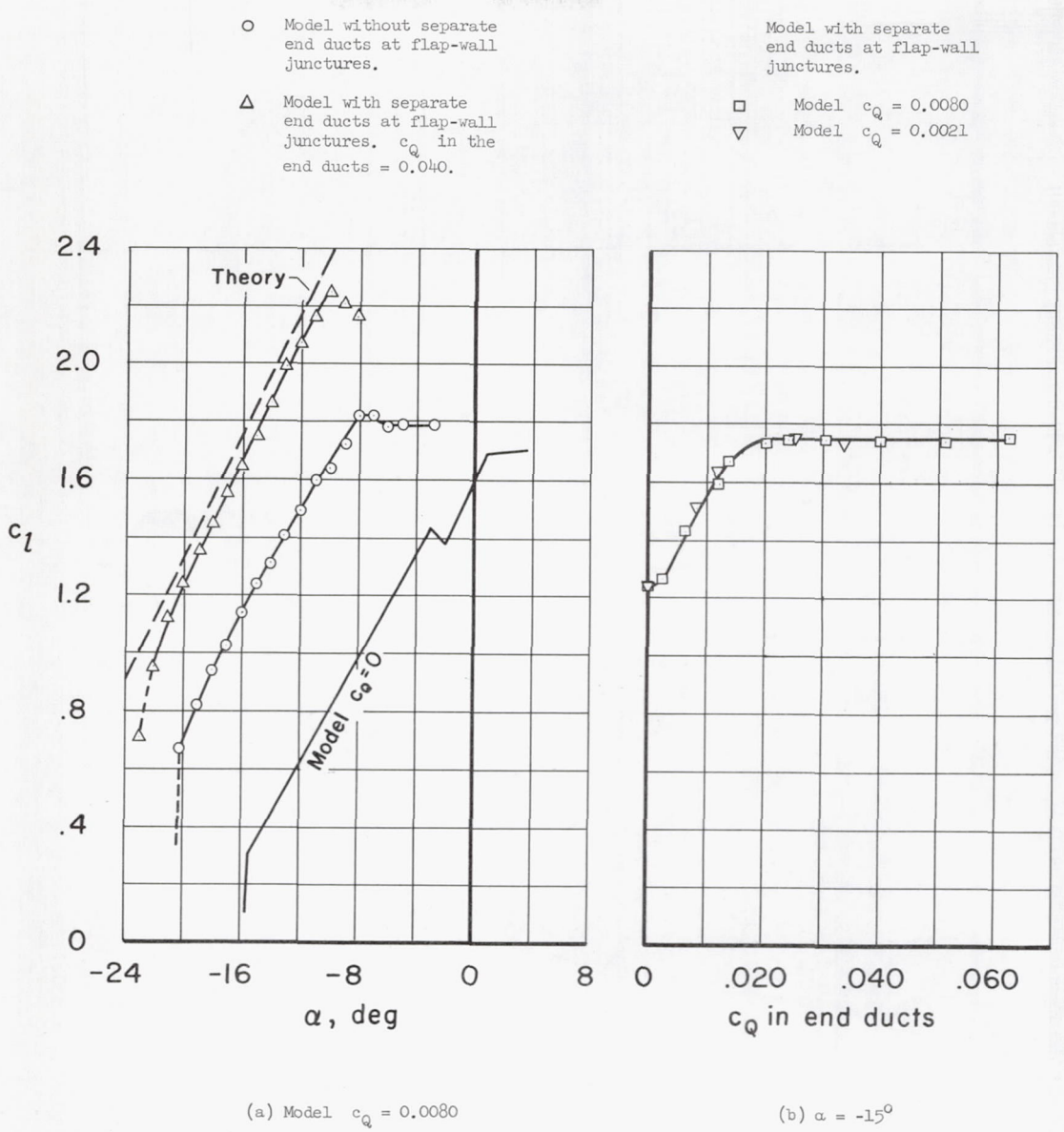

(a) Model c_Q = 0.0080 (b) $\alpha = -15^\circ$

Figure 7.- Effect of increased suction at flap-wall junctures on section lift coefficient.

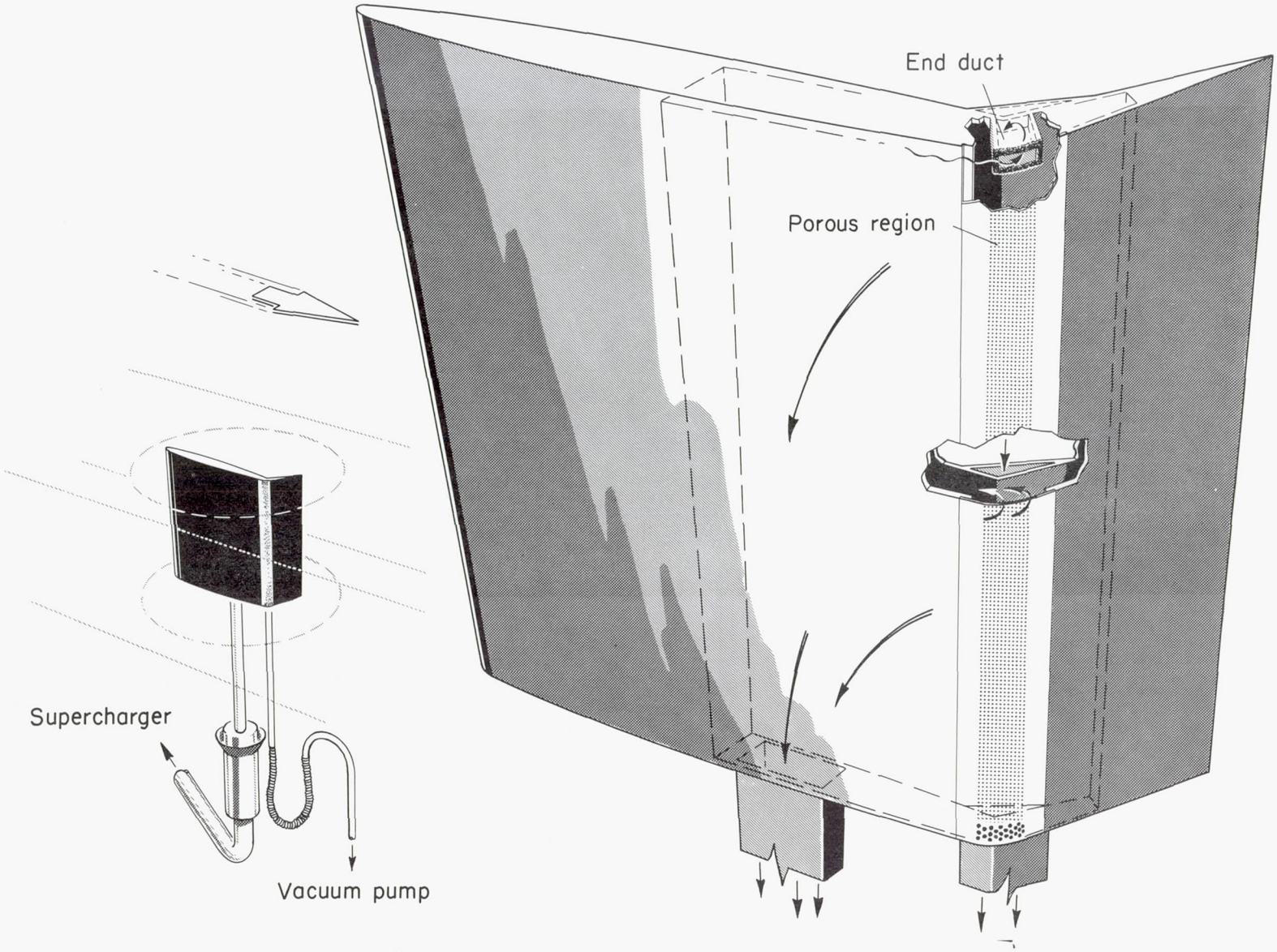

Figure 8.- Construction details of the NACA 0006 airfoil model with perforated surface on the flap for area suction studies.

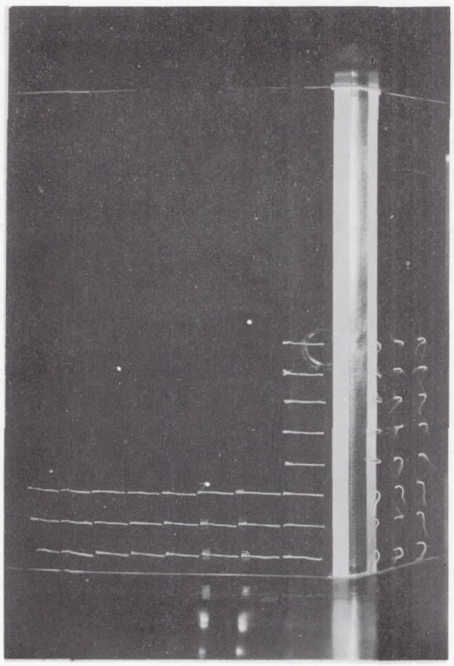

(a) $c_Q = 0$

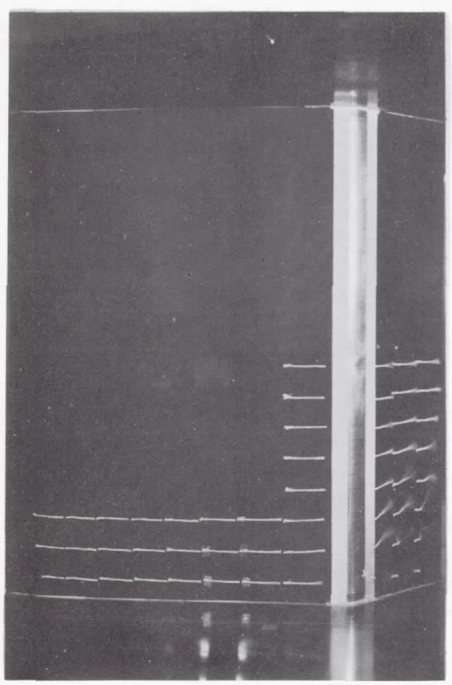

c_Q end ducts = 0

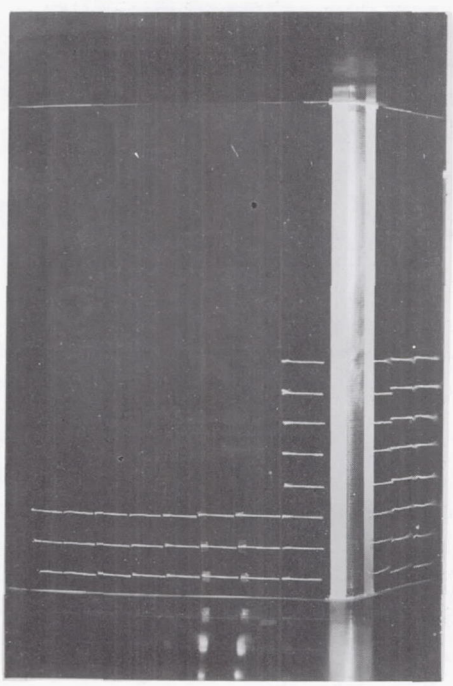

c_Q end ducts = 0.04

(b) Model $c_Q = 0.0050$

Figure 9.- Tuft studies over the upper surface of the model; $\alpha = -15^\circ$.

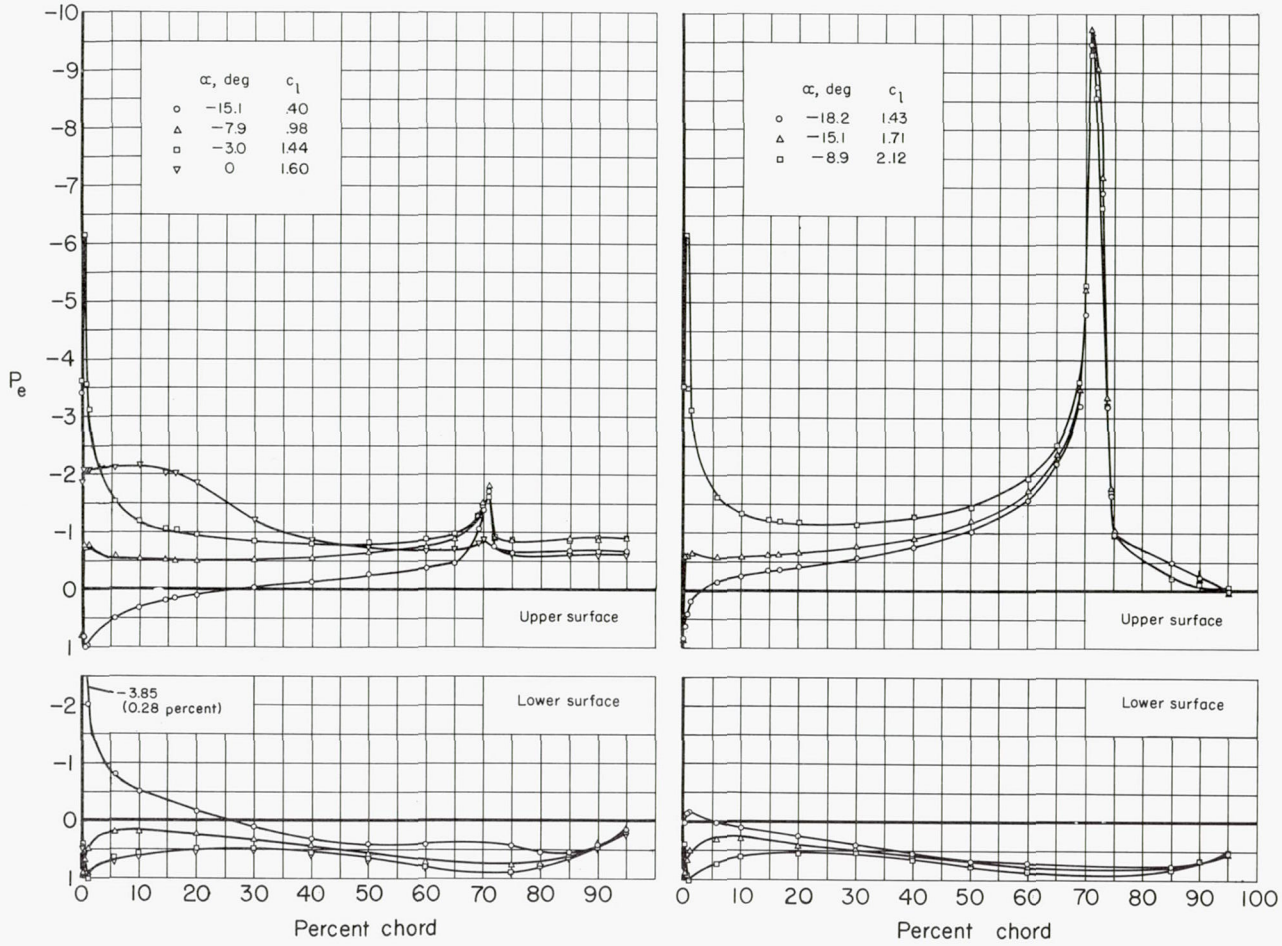

Figure 10.- Typical pressure distribution over the model with suction applied in the hinge-line region on the flap; uniform arrangement of permeability in the porous region.

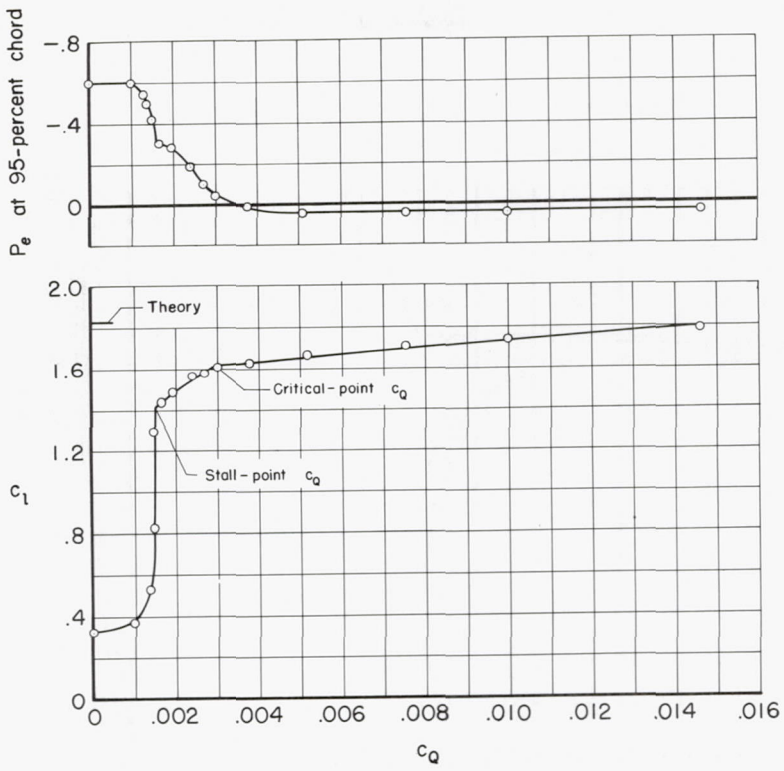

(a) $\alpha = -15°$

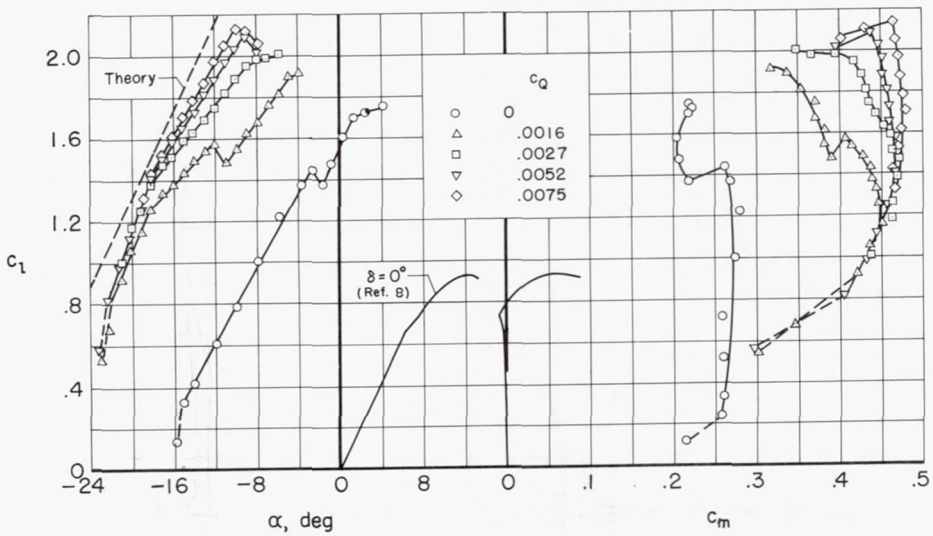

(b) Lift and moment characteristics.

Figure 11.- Typical aerodynamic characteristics of the model with suction applied in the hinge-line region on the flap; uniform arrangement of permeability in the porous region.

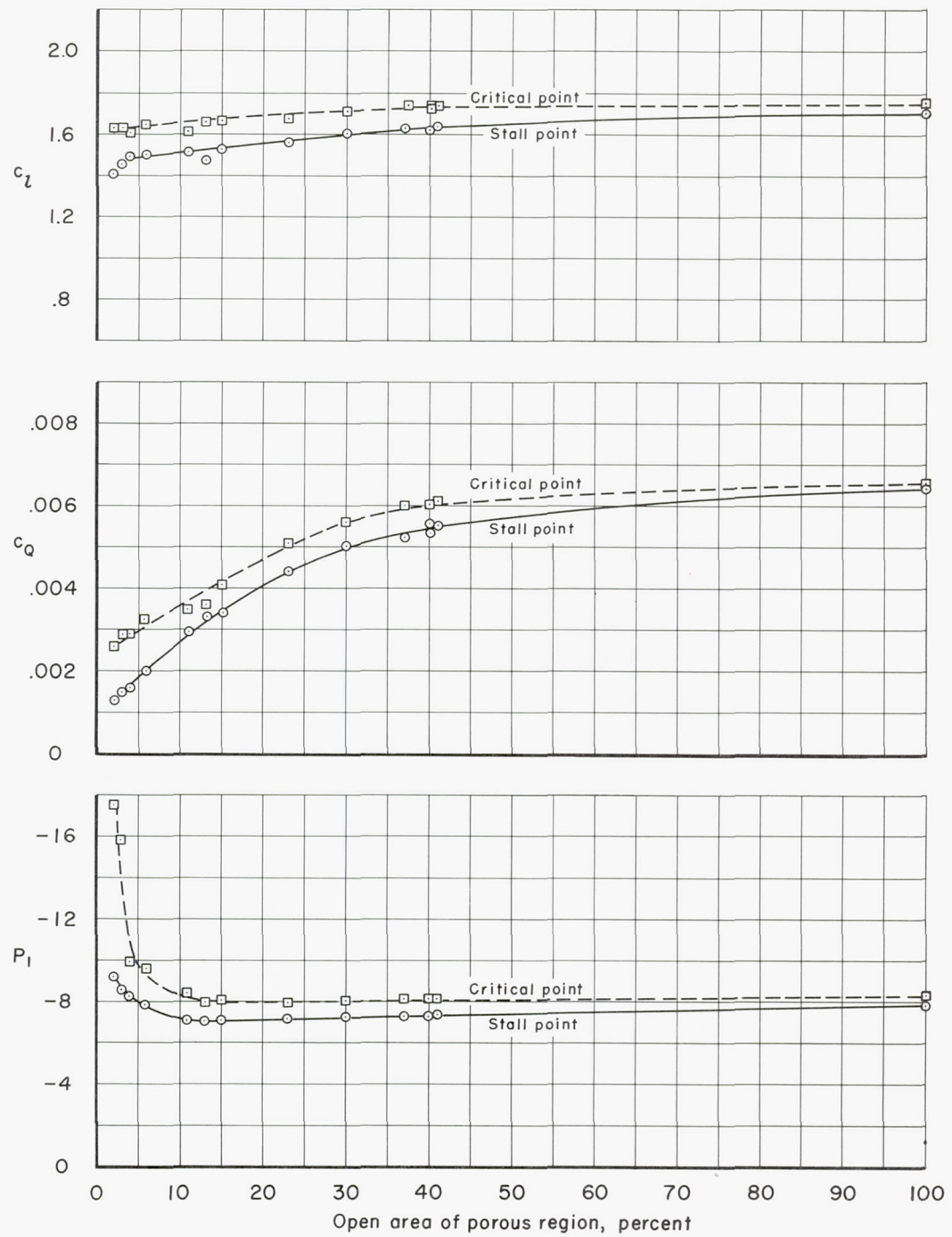

Figure 12.- Stall-point lift and flow characteristics of the model with uniform arrangements of permeability in the porous region; perforation patterns with $x/d \approx s/d$; $\alpha = -15^{\circ}$.

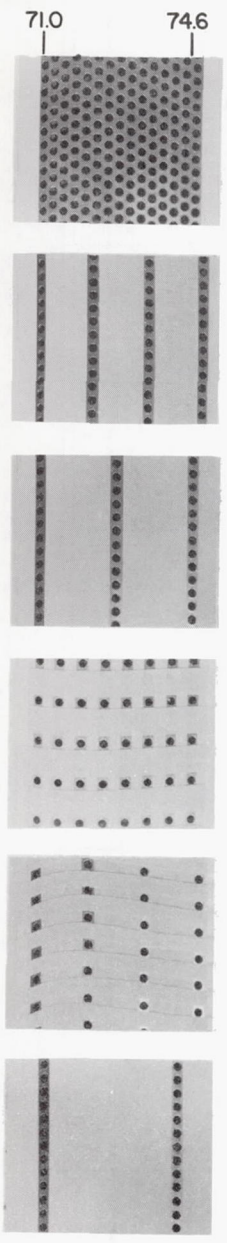

Uniform permeability, from figure 12

Discrete permeability

	Surface	Percent open	s/d	z/d	Suction velocity at trailing edge of porous region, fps	c_l
○	13	40	1.3	1.5	126	1.62
△	13-A	10.6	6.5	1.5	28	1.57
□	13-B	8.0	9.1	1.5	25	1.55
▽	13-C	7.2	2.6	4.6	22	1.53
◇	13-D	5.3	6.5	3.0	15	1.54
⌂	13-E	5.3	15.6	1.5	16	1.56

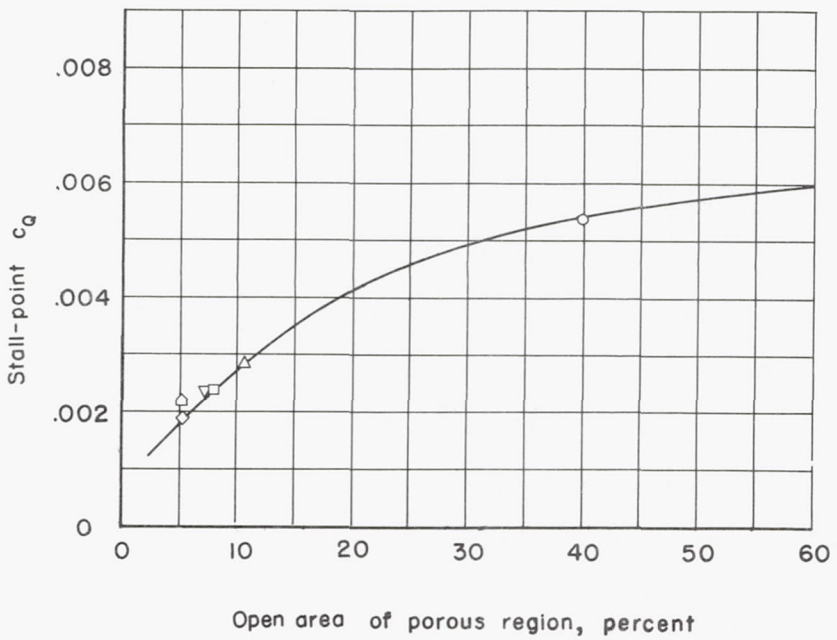

Figure 13.- Stall-point section flow characteristics of the model with discrete arrangements of permeability in the porous region; $\alpha = -15^\circ$; hole diameter = 1/8 inch.

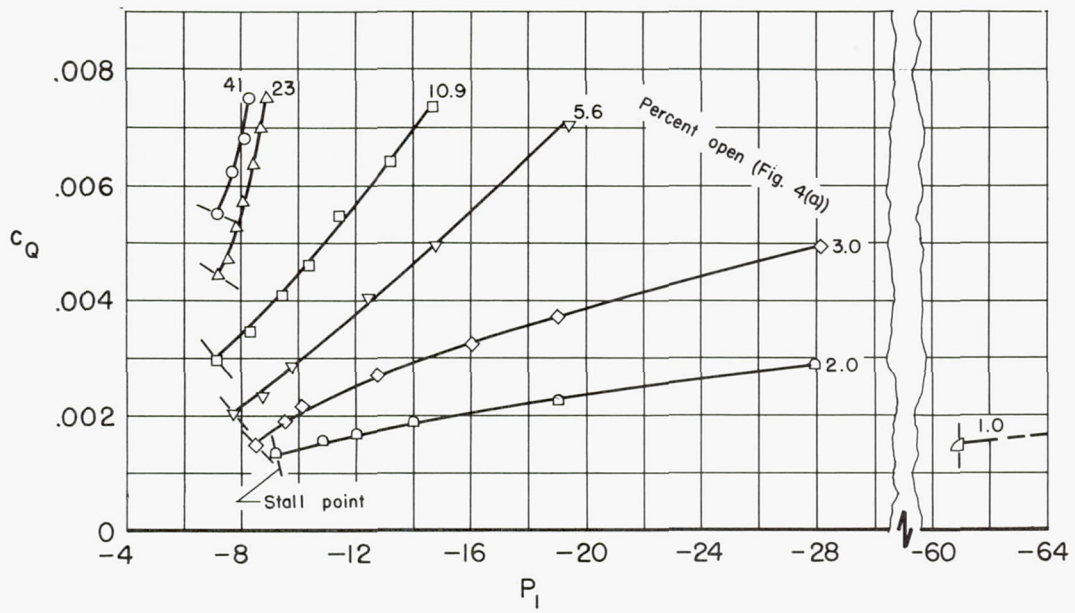

(a) Uniform permeability.

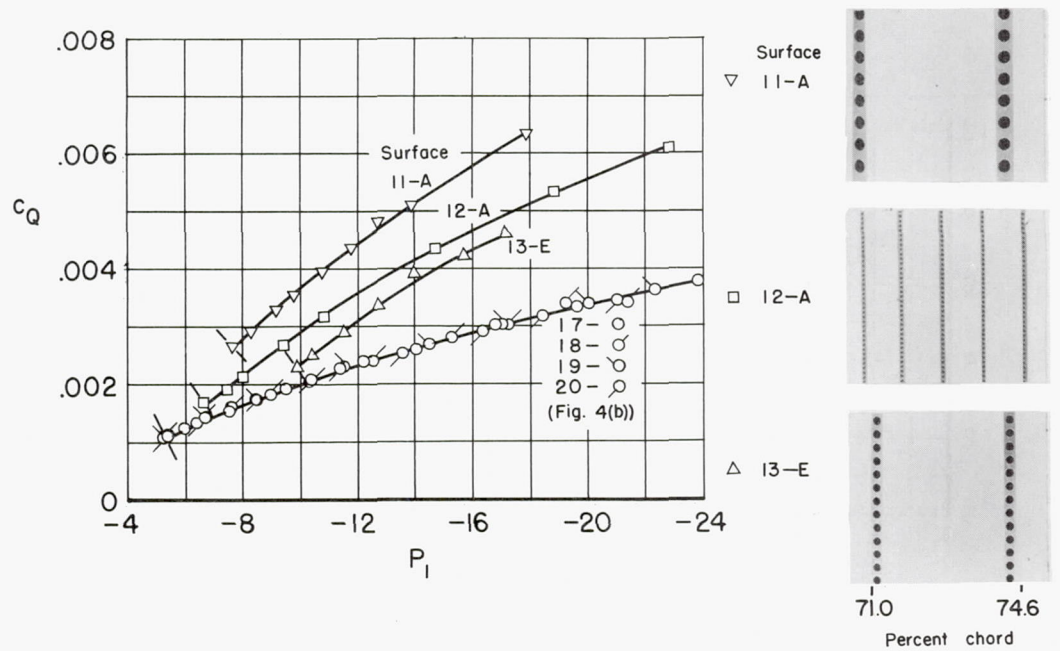

(b) Gradient and discrete permeability.

Figure 14.- Variation of section flow coefficient with plenum-chamber pressure coefficient for the model with various arrangements of permeability in the porous region; $\alpha = -15^{\circ}$.

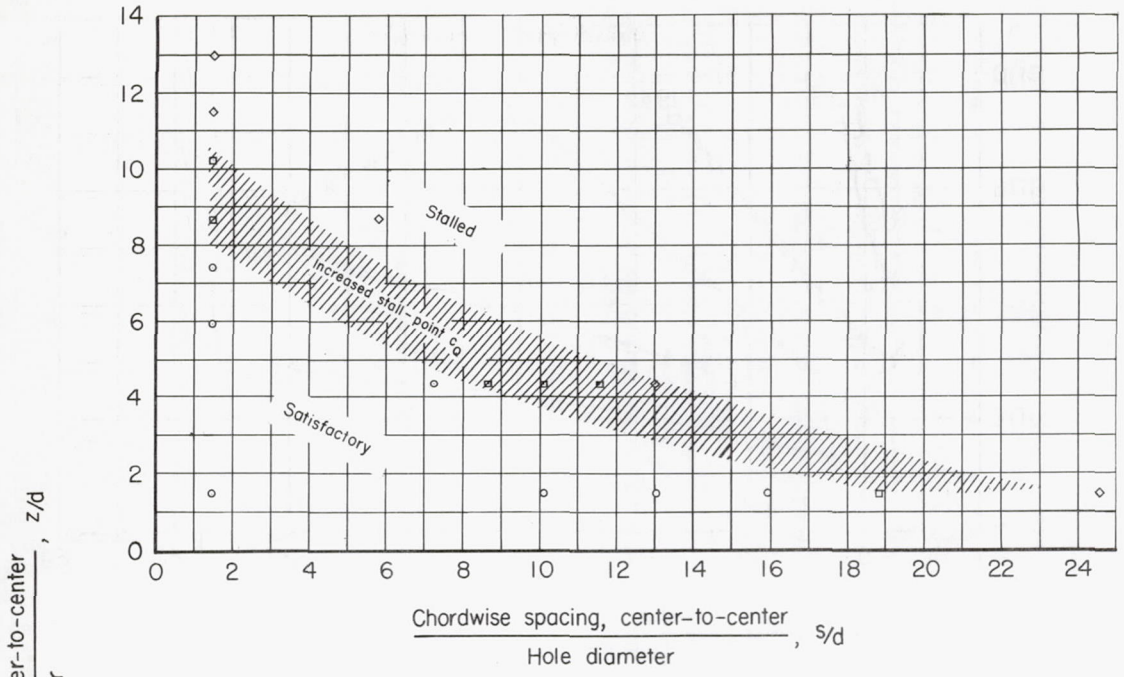

(a) Hole diameter of 0.045 inch, surface 12.

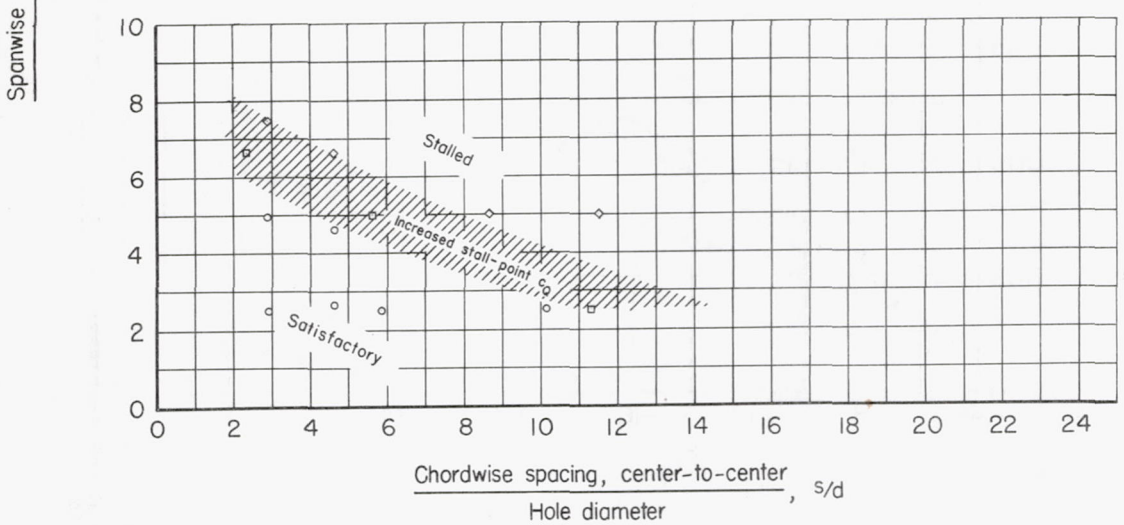

(b) Hole diameter of 0.094 inch, surfaces 7 and 8.

Figure 15.- Range of perforation patterns satisfactory for use as the surface of the porous region of the model; discrete arrangements of permeability; $\alpha = -15^{\circ}$.

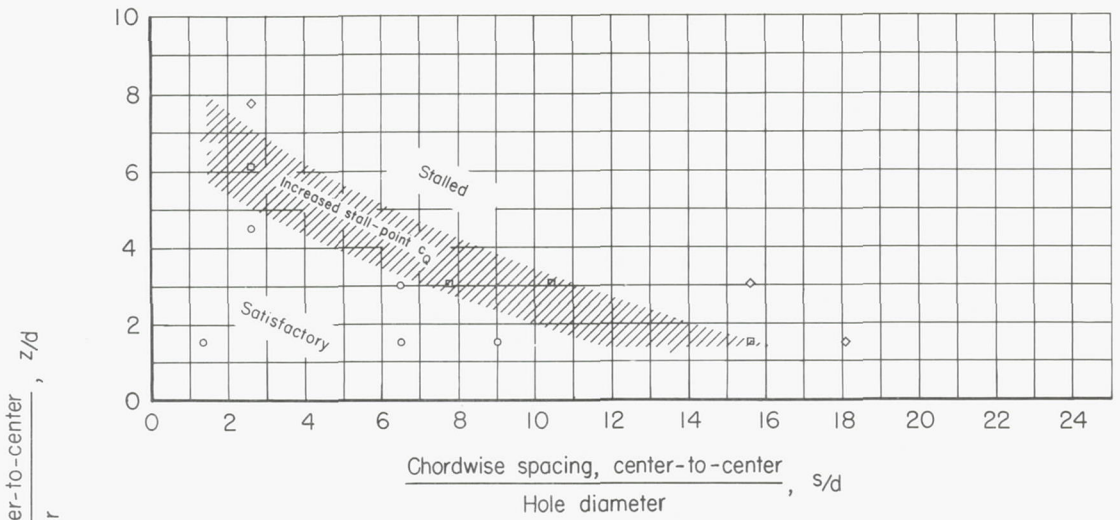

(c) Hole diameter of 0.125 inch, surface 13.

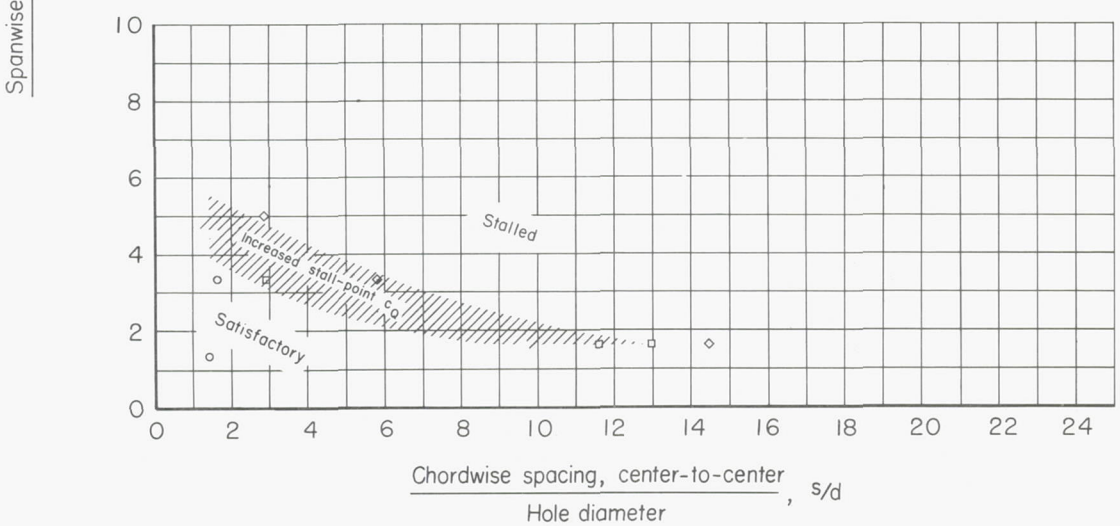

(d) Hole diameter of 0.187 inch, surface 11.

Figure 15.- Concluded.

Porous material: Composite assembly

○ Surface 13

□ Surface 16

◇ Surface (Ref. 1) having 4,225, 0.006-inch square holes/sq in.

Porous material: Perforated sheet

△ Surfaces 17, 18, 19, 20

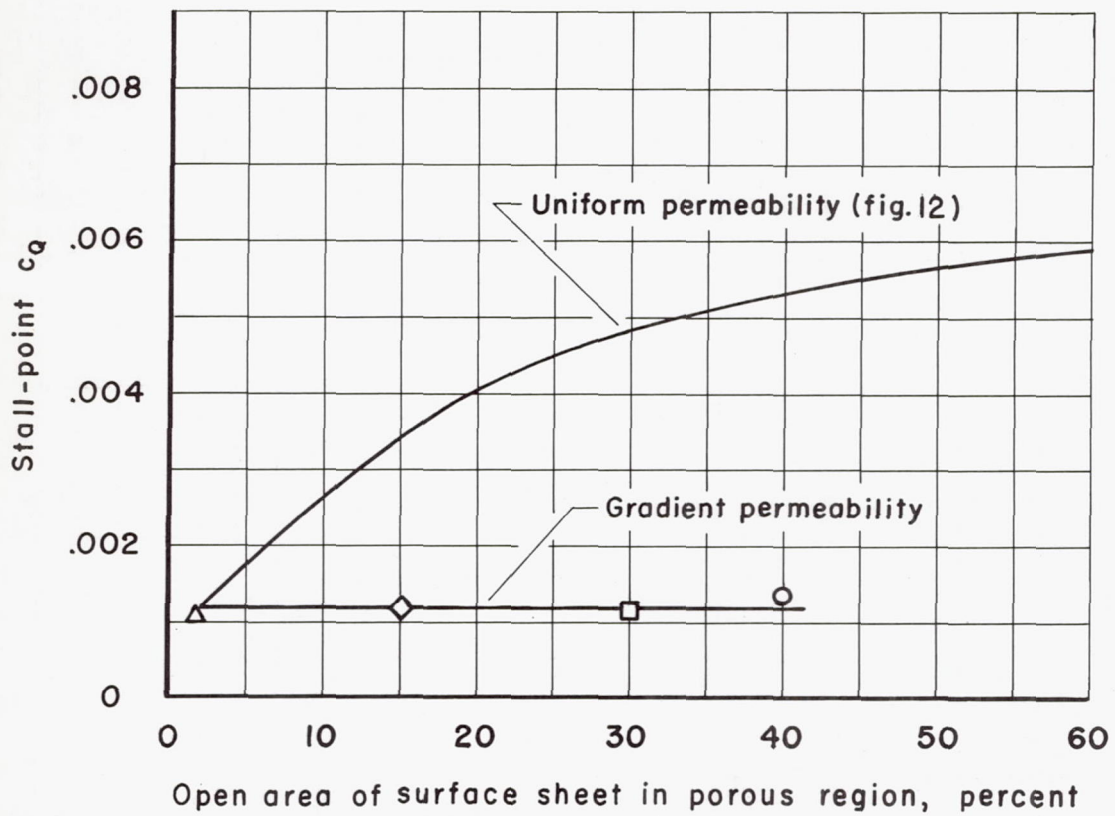

Figure 16.- Stall-point section flow characteristics of the model with a gradient arrangement of permeability in the porous region; $\alpha = -15^{\circ}$.

	Surface	Percent open	Stall-point c_q	Suction velocity at trailing edge of porous region, fps
○	4	3.0	0.0015	9
△	6	5.6	.0021	17
□	8	13.0	.0033	37
▽	10	23.0	.0045	69
◇	15	41.0	.0056	126
◿		100.0	.0064	304

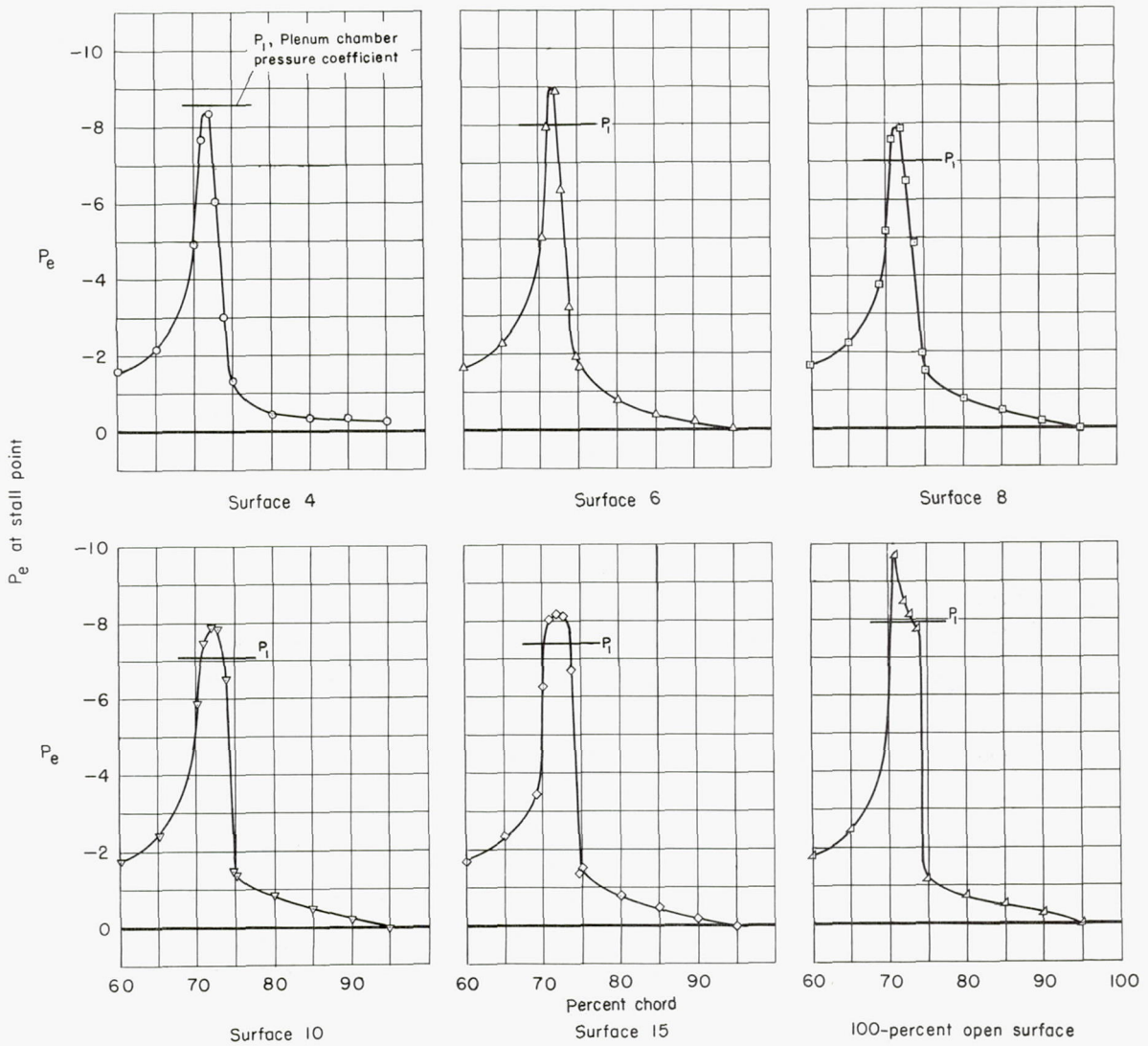

Figure 17.- Stall-point pressure distribution over the flap with various arrangements of uniform permeability in the porous region; $\alpha = -15^{\circ}$.

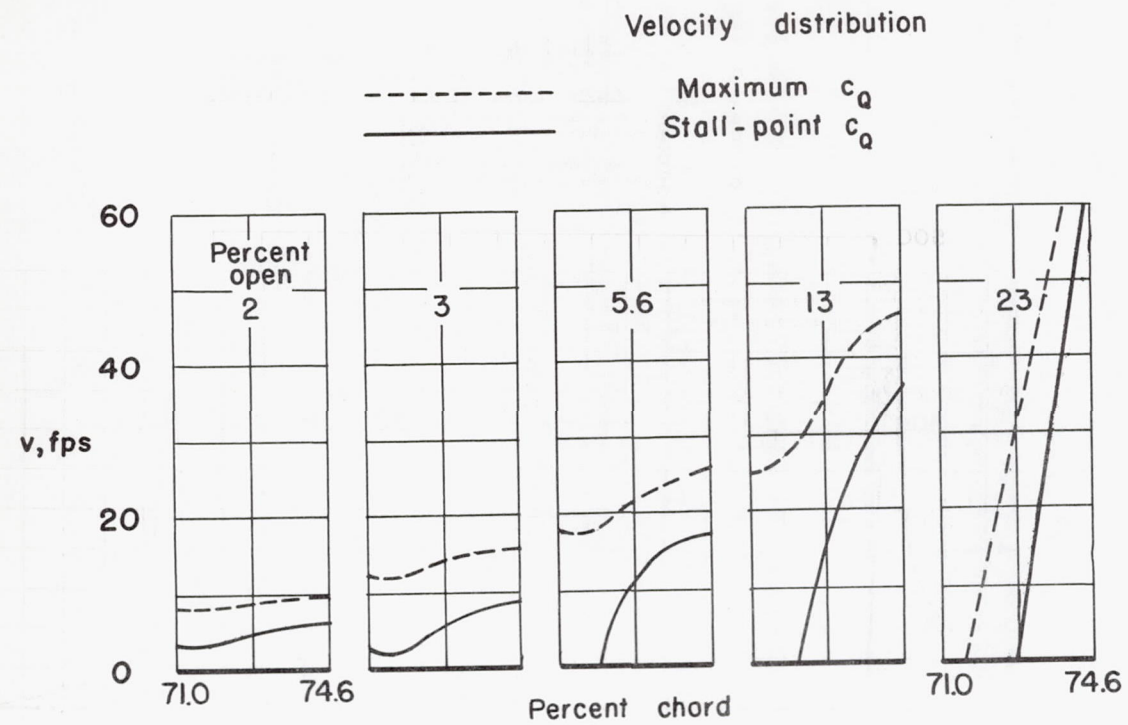

(a) Uniform permeability.

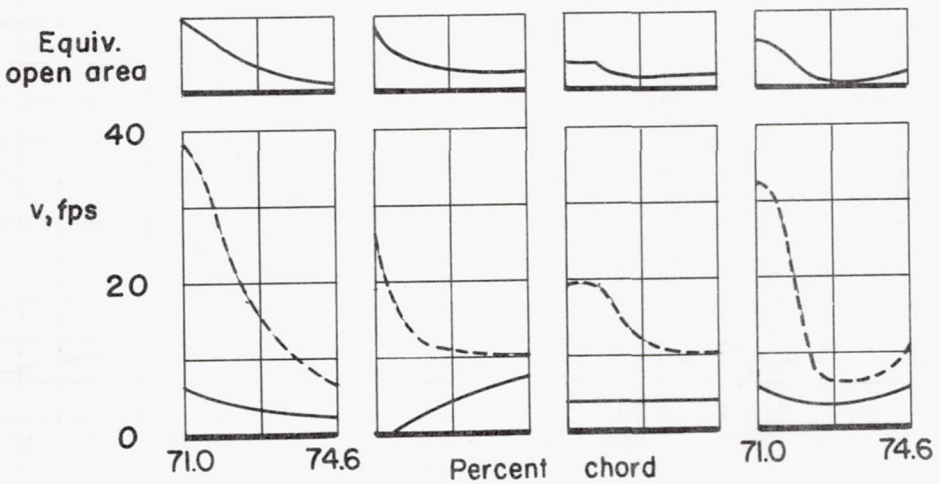

(b) Gradient permeability;
Surface 10 with resistance backing.

Figure 18.- Suction velocity distributions for various arrangements of permeability; $\alpha = -15^{\circ}$.

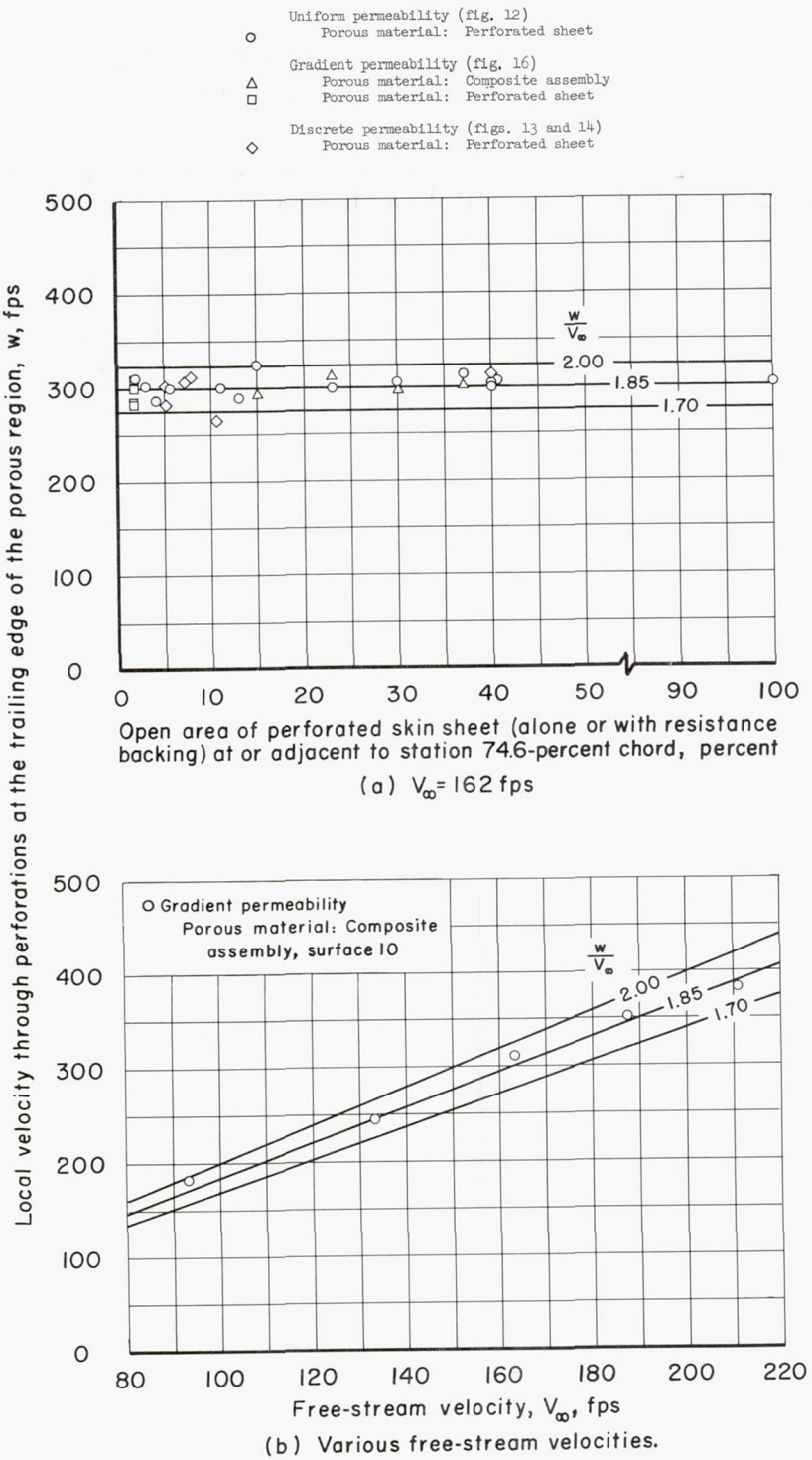

Figure 19.- Measured values of the local suction velocities through the perforations at the trailing edge of the porous region for stall-point conditions; $\alpha = -15^{\circ}$.